Paper 239

©Civil-Comp Press, 2012
Proceedings of the Eleventh International Conference
on Computational Structures Technology,
B.H.V. Topping, (Editor),
Civil-Comp Press, Stirlingshire, Scotland

Theoretical and Experimental Analysis of Tensegrity Structures

S. Kmet and P. Platko
Faculty of Civil Engineering
Technical University of Kosice, Slovak Republic

Abstract

A newly developed adaptive tensegrity module in the form of a double symmetrical pyramid which has the ability to alter its geometrical form and pre-stress properties in order to adapt its behaviour in respond to the current loading conditions is presented in this paper. The system consists of eight pre-stressed cables, four circumferential compressed rods and the central compressed rod designed as an actuator. Three types of the tests were carried out: a pre-stressing test, a static loading test and an adaptation test to confirm the required functionality of the developed adaptive system and the correctness of the proposed closed-form and discrete computational models and control commands.

Keywords: adaptive tensegrity module, octahedral cell, actuator, sensors, test equipment, tests, control commands, closed-form solution, finite-element analysis.

1 Introduction

Lightweight self-stressed tensegrity systems, that are composed of tensioned members (cables) and compressed members (struts), offer an economical and efficient alternative to many classical civil-engineering and aerospace structures. Their use is very promising in projects that require active or deployable systems. Tensegrity structures have been intensively studied since they appeared in the fifties and their applications have been extended from art and architecture to other areas including aerospace structures, robotics and cell mechanics.

A tensegrity system was originally developed in 1948 by the sculptor Kenneth Snelson in the form of a tensegrity tower and in the early sixties patents were simultaneously deposited by Richard Buckminster Fuller in the USA and David Georges Emmerich in France (see for example the monographs by Fuller [1], Pugh [2], Motro [3] and Skelton and de Oliveira [4]).

Geometry of the tensegrity system and initial pre-stresses introduced into the members of the tensegrity system at its self-equilibrium state have a significant influence on the behaviour of the loaded structure and greatly contribute to its stiffness and stability. In contrast with cable and membrane structures, tensegrities do not need massive anchorages of large tensile forces due to their self-stress characteristic.

Many regular and also non-regular tensegrity systems have been developed in recent years and a considerable research related to their geometry, form-finding and architecture have been performed. Murakami and Nishimura [5] presented initial equilibrium and modal analyses of cyclic right-cylindrical tensegrity modules with an arbitrary number of stages. Zhang *et al*. [6] presented the form-finding of non-regular tensegrity structures with a numerical approach based on the dynamic relaxation method with kinetic damping. New tensegrity configurations in more intricate and creative forms can be obtained by this method. Rieffel *et al.* [7] introduced an evolutionary algorithm which produces large and complex irregular tensegrity structures, and demonstrated its efficacy and scalability relative to previous methods. Tran and Lee [8] proposed an efficient and robust numerical method for searching self-equilibrium configurations of tensegrity structures based only on topology and type of members (either tensioned or compressed member). Xu and Luo [9] presented a detailed investigation on a multistable tensegrity structure whose basic stable configuration corresponds to the expanded octahedron tensegrity. Using an evolutionary form-finding scheme, together with the dynamic relaxation method, two other self-equilibrated configurations with higher strain energies were found and verified by physical models. This study provides a theoretical basis for the further applications of multistable tensegrity systems. Tibert [10] investigated deployable structures based on the tensegrity concept for space applications. Saitoh *et al.* [11] , through loading a tensegrity arch, showed that a developed analytical model of the arch was able to correctly reflect its real behaviour. Wu and Sasaki [12] investigated the static and dynamic behavior of a cable-stiffened arch by means of numerical and experimental methods.

Tensegrity structures are sensitive to asymmetric loads and small environmental changes. Active tensegrity systems equipped with sensors and actuators provide the potential to control their shape and adapt to changing load and environmental conditions (Shea *et al.* [13]).

Development of adaptive tensegrity structures has been a subject of research since the end of last century. This area is studied systematically at Swiss Federal Institute of Technology (EPFL) where a full-scale prototype of an adjustable tensegrity system has been built and tested (Fest *et al.* [14]). The structure consisted of three modules and its adjustments were made manually. Building on a previous study of an adjustable structure, Fest *et al.* [15] described geometric active control of an enlarged tensegrity structure consisted of five modules with ten actuators in the form of telescopic struts. Actuators consisted of the electromechanical jacks which produce linear energy by rotary energy. Authors developed the stochastic search algorithm for an identification of control commands. In many cases an active control of tensegrity structures is studied mainly through simulation and numerical experiments where most work is focused on dynamic behaviour and vibration control.

A developed new adaptive tensegrity system which has the ability to alter its geometrical form and stress properties in order to adapt its behaviour in response to the current loading conditions is presented in the paper. Results of the experimental and theoretical analyses of the developed system are briefly characterized.

2 Characteristics of structural properties of an adaptive tensegrity module

The full-scale prototype of an adaptive tensegrity module was designed and built at the Laboratory of Structural Engineering of Faculty of Civil Engineering of the Technical University of Kosice. The elementary shape of the tensegrity module is an octahedral cell in the form of a double symmetrical pyramid with a square base as is shown in Figure 1.

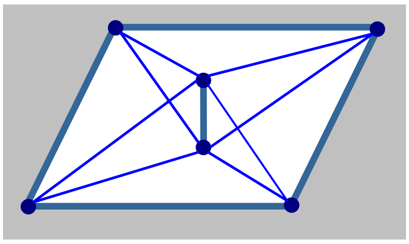

Figure 1: Elementary shape of the tensegrity module.

Theoretical base plan dimensions are 2000x2000 mm and a height of one pyramid is 400 mm. Thus, the distance between the peaks of the both pyramids is 800 mm. This basic bearing structural system consists of eight tension members (cables) and five compression members (struts). All the members are mutually connected in nodes by hinge joints. Four of the five compressed members form a square perimeter of the tensegrity module and the fifth middle member is designed as an actuator. This active telescopic strut is used to modify the geometry and self-stress of the tensegrity system. The basic members and geometry of the tensegrity module are shown in Figure 2.

The four circumferential struts of the tensegrity system are created as circular hollow sections of $51/3{,}2$ mm (external diameter/web thickness) and are made from steel $S235$. The cross-sectional area of the tubular struts is $A_s = 475{,}9\ mm^2$ and Young's modulus of elasticity is $E_s = 210000\ Nmm^{-2}$. The theoretical length of the struts is $L_s = 2000\ mm$. Strand ropes of construction 7 x 7 (7 strands with 7 wires per strand) with a nominal diameter of 6,0 mm were used for tensile cables. Cables were made from the stainless austenitic steel 1.4401. The cross-sectional area of the bottom and top cables is $A_{c,b} = A_{c,t} = 15{,}2\ mm^2$ and Young's modulus of elasticity is $E_{c,b} = E_{c,t} = 120000\ Nmm^{-2}$. Cables are terminated with swaged terminals with pin connectors. The characteristic value of the breaking force of the tension components is $F_{uk} = 20100\ N$. The theoretical length of the bottom and top cables is $L_{c,b} = L_{c,t} = 1469{,}69\ mm$. The ground plan diagonal length of cables is $L_d = 2824{,}42\ mm$.

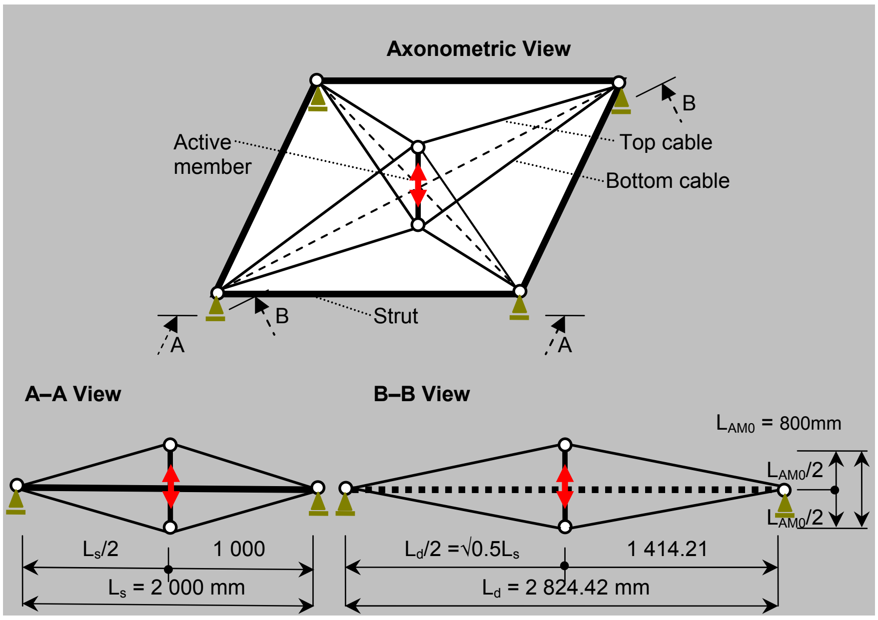

Figure 2: Basic members and geometry of the tensegrity module.

The hydraulic actuator is the part of the central compressed rod of the tensegrity system with the theoretical length of $L_{AM,0} = 800\ mm$. The actuator consists of a rectilinear hydraulic motor with an inductive position sensor embedded in the piston rod. This sensor enables to record the current force F_{AM} in the action member together with the corresponding current position Δ_{AM}. Detailed view of the actuator is shown in Figure 3.

Figure 3: View of an action member (AM).

Considerable attention has been given to the design and implementation of details of joints and connections of forming members of the tensegrity system. The aim was to achieve a perfect hinge interconnection between members and thus perfectly capture the principles of the action of tensegrity structures. Cable members terminated by moulded terminals with adjustable parts are attached to the circumferential compressed struts and to the top and bottom edge of the action member by spherical pins. Consequently, these connections create total hinges (the possibility of rotation in all directions). Connections of cable members with embedded force transducers requested the special arrangements of details. Characteristic details are shown in Figure 4.

(a)

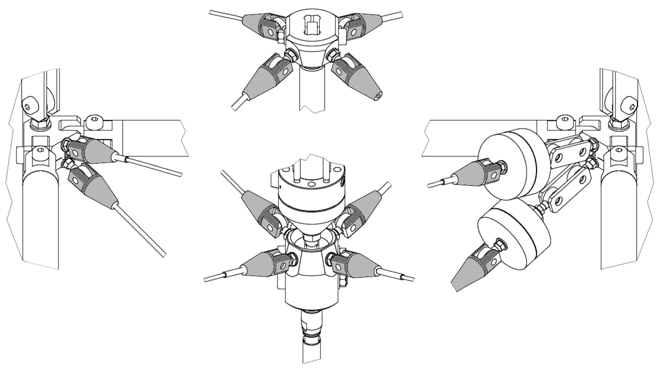

(b)

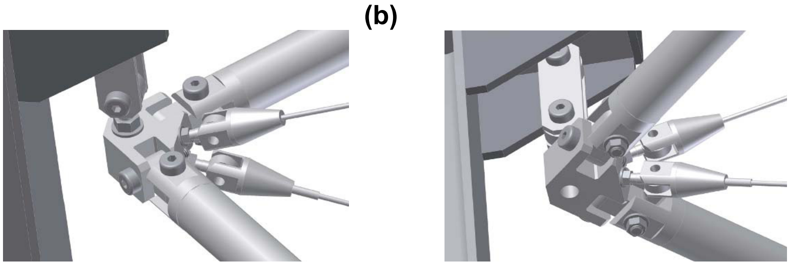

Figure 4: Design and visualisations of the details of attachments of cable members to the circumferential compressed struts and to the top and bottom edge of the action member by spherical pins (a) and visualisations (b).

3 Control of an adaptive tensegrity module

3.1 Monitoring and adaptation strategy

The tensegrity module is equipped with the sensors and actuator consequently the geometry and prestress and thereby the behaviour of the system can be adapted. In addition to primary sources of the signal from the action member (recording of the force in the actuator and its movement) also the ten following signal sources were installed onto the tensegrity module (Figure 5): four force transducers placed in the two bottom and in the two top cable members (force transducers FT 1 to FT 4) and six strain gauges mounted on the circumferential compressed struts (strain gauges SG 1 to SG 6). Force transducers with a nominal load capacity of 10,0 kN directly sense current forces in the cable members and strain gauges sense strains of the compressed struts.

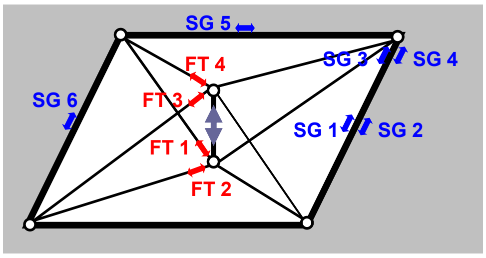

Figure 5: Positions of measuring accuracy elements: force transducers (FT) and strain gauges (SG).

The goal of the form adjustment of the tensegrity module is to maintain pre-stresses of the top cables at required levels (control of slackening effects), control forces in the cables and thereby also a deformation of the structure. A finding of an adjustment command is in this case not so complicated and straightforward. Consequently, from the closed-form solution of the tensegrity module the relationship between inputs and outputs can be defined.

Continuous monitoring and measurement enable one to detect any changes in the structural behaviour. The adaptation procedure can be divided into following steps: (i) The tensegrity module is activated by the actuator and the required initial pre-stress is introduced to the individual cables of the system. The current force and movement of the actuator are measured and recorded. (ii) The initial pre-stress state of the tensegrity structure is measured. Forces in cables and struts are measured by load cells and strain gauges, respectively. (iii) The tensegrity module is loaded and the actual state of stress is measured. Actual forces obtained from sensors are compared with the defined limiting values and the reliability criteria of the system are advised. (iv) If the criteria of reliability defined for the tensegrity system are exceeded a structural analysis (the closed-form or discrete analysis) is performed to provide a control command for an adjustment of the actuator (a control command for a required extension or contraction of the active member). (v) After the active member is adjusted hence the tensegrity system is adapted to the imposed load the current response of the structure is measured and criteria of reliability are verified. In the case that the required criteria are fulfilled the adaptation of the system for the given load is finished. (vi) If load is changed the above-mentioned procedure is repeated.

Actual values of signals from individual sensors are continuously monitored and at the any change they are automatically recorded and evaluated using a computer.

3.2 Adaptation of a tensegrity module

3.2.1 A pre-stressed state

In order to obtain the required overall stability and stiffness of the tensegrity module initial pre-stressing forces are introduced into the bottom and top cables of the system. Pre-stress is introduced into the each cable by a corresponding movement of the actuator (an activation of the cable members by an elongation of the action member). The level of initial pre-stress has a significant influence on the behaviour of the structure under variable external actions.

The required initial pre-stress of the tensegrity system is obtained by the corresponding movement (elongation) of the active member when the initial pre-stressing forces are introduced into the cable members.

The required displacement of the active member $\Delta_{AM,i}$ is obtained in the form

$$\Delta_{AM,i} = 2L_{c0b,0t}\left(\cos(\alpha_{0b,0t}+90°)+\sqrt{\cos^2(\alpha_{0b,0t}+90°)+\frac{N_{c0b,0t}}{E_{cb,t}A_{cb,t}}\left(\frac{N_{c0b,0t}}{E_{cb,t}A_{cb,t}}+2\right)}\right) \quad (1)$$

where L_{c0b} and L_{c0t} are the initial theoretical lengths of the bottom and top cables, respectively, α_{0b} and α_{0t} are the angles which contain the cable lengths L_{c0b} and/or L_{c0t} with the horizontal axis, N_{c0b} and N_{c0t} are the initial pre-stressing forces in the bottom and top cable, E_{cb} and E_{ct} are the modules of elasticity of the bottom and top cables, respectively and A_{cb} and A_{ct} are the cross-sectional areas of the bottom and top cable.

Initial lengths and angles can be calculated from the following expressions (Figure 6)

$$L_{c0b} = L_{c0t} = \sqrt{0{,}5\left(L_s^2+0{,}5L_{AM0}^2\right)}$$

$$\alpha_{0b,0t} = \sin^{-1}\left(\frac{0{,}5L_{AM0}}{L_{c0b,0t}}\right) = \sin^{-1}\left(\frac{0{,}5L_{AM0}}{\sqrt{0{,}5\left(L_s^2+0{,}5L_{AM0}^2\right)}}\right) \text{or}\ \alpha_{0b,0t} = \tan^{-1}\left(\frac{0{,}5L_{AM0}}{\sqrt{0{,}5L_s}}\right) \quad (2)$$

where L_{AM0} is the initial length of the active member and L_s is the length of the circumferential struts.

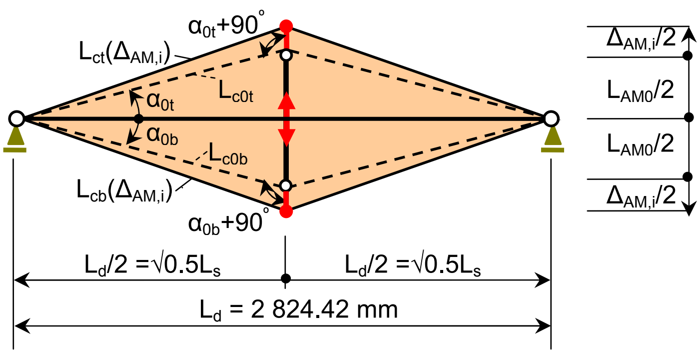

Figure 6: Geometry of the module before and after prestressing.

Using notation as in Figure 6, the following expressions for the lengths $L_{cb}(\Delta_{AM,i})$ and $L_{ct}(\Delta_{AM,i})$ after an application of the law of cosines are obtained

$$L_{cb,t}\left(\Delta_{AM,i}\right)=\sqrt{L_{c0b,0t}^{2}+\frac{1}{4}\Delta_{AM,i}^{2}-L_{c0b,0t}\Delta_{AM,i}\cos\left(\alpha_{0b,0t}+90°\right)} \tag{3}$$

where $L_{cb}\left(\Delta_{AM,i}\right)$ and $L_{ct}\left(\Delta_{AM,i}\right)$ are the lengths of the bottom and top cables after deformation when the active member is moved.

3.2.2 A load state

The basic condition for the reliability of the tensegrity system is the existence of tensile forces in cable members during the required service life of the structure, which can be expressed in the form

$$N_{cb,t,j}(t)>0 \tag{4}$$

where $N_{cb,j}(t)$ and $N_{ct,j}(t)$ are the axial forces in the bottom and top cables of the loaded system at the time t, respectively. Generally, slackening of cables (mainly of the top cables) of the system may be caused by several influences as are an external variable action, creep of cables under the long-term load (stress relaxation), temperature effects, an additional elongation of the cable after deformation at the point of connection and likewise.

If the condition (4) is not fulfilled or the decrease of the pre-stressing forces in the top cables of the system due to the applied load $P_{LC,j}$ (generated by the load cylinder LC) at the j state is significant the active member must be elongated in order to generate an increase of the forces in the top cables (Figure 7a). The required movement of the active member (control command) $\Delta_{AM,i+1}$ necessary to obtain the target increased forces $N_{ct,j}^{tar}$ is calculated from the following relationship

$$\Delta_{AM,i+1}=2L_{ct,j}\left[\cos\left(\alpha_{t,j}+90°\right)+\sqrt{\cos^{2}\left(\alpha_{t,j}+90°\right)+\frac{N_{ct,j}^{tar}}{E_{ct}A_{ct}}\left(\frac{N_{ct,j}^{tar}}{E_{ct}A_{ct}}+2\right)}\right] \tag{5}$$

where $L_{ct,j}$ is the length of the top cables after deformation under the load $P_{LC,j}$ given by the relation

$$L_{ct,j}=\sqrt{\left(\sqrt{0,5L_{s}}\right)^{2}+\left(d_{t}-w_{j}\right)^{2}}=\sqrt{0,5L_{s}^{2}+\left(d_{t}-w_{j}\right)^{2}}=\sqrt{0,5L_{s}^{2}+\left(0,5L_{AM,i}-w_{j}\right)^{2}} \tag{6}$$

where w_j is the vertical deflection at the midpoint of the tensegrity system under the load $P_{LC,j}$ (obtained from the structural analysis or by the measuring), $d_t=0,5L_{AM,i}$ is the camber of the top cables and $L_{AM,i}=L_{AM0}+\Delta_{AM,i}$ is the length of the active member after the initial pre-stressing forces were introduced into the system (see Eq. (1)). The angle $\alpha_{t,j}$ is given by the formula

$$\alpha_{t,j}=\sin^{-1}\left(\frac{d_{t}-w_{j}}{L_{ct,j}}\right)=\sin^{-1}\left(\frac{0,5L_{AM,i}-w_{j}}{L_{ct,j}}\right) \tag{7}$$

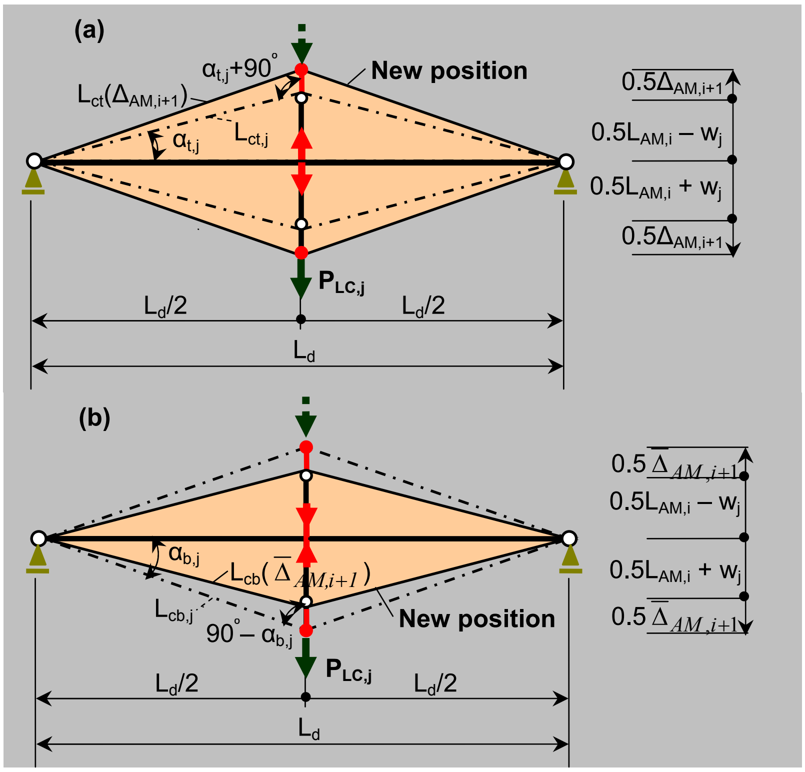

Figure 7: Geometry of the module: an elongation (a) and shortening (b) of an AM.

For the ultimate limit state (ULS) is verified that [16]

$$F_{Ed} \leq F_{Rd} \tag{8}$$

where $F_{Ed} = N_{cb,j}$ is the design value of the axial cable force in the bottom carrying cables from the corresponding load $P_{LC,j}$ of the tensegrity system and F_{Rd} is the design value of the tension resistance of the cable. The value of $N_{cb,j}$ is obtained from closed-form (see Section 5) or FE analysis (see Section 6) and also by measuring the tensegrity system under corresponding loading. The design value of the tension resistance F_{Rd} of the cable is taken as

$$F_{Rd} = \min\left\{\frac{F_{uk}}{1{,}5\gamma_R}; \frac{F_{0,2k}}{\gamma_R}\right\} \tag{9}$$

where F_{uk} is the characteristic value of the breaking strength of the cable, $F_{0,2k}$ is the characteristic value of the $0{,}2\%$ proof strength determined from tests and γ_R is the partial factor, whose value is dependent on whether or not measures were applied at the cable ends to reduce bending moments from cable rotations. F_{uk} is calculated as

$$F_{uk} = F_{min} k_e \tag{10}$$

where F_{min} is the characteristic value of the minimal breaking strength of the cable and k_e is the loss factor depending up the type of the end termination of the cable.

If the condition (8) is not fulfilled the action member must be shortened in order to achieve a decrease of the forces in the bottom cables (Figure 7b). The required movement of the action member (control command) $\overline{\Delta}_{AM,i+1}$ necessary to obtain the target reduced forces $N_{cb,j}^{tar}$ is calculated from the following relationship

$$\overline{\Delta}_{AM,i+1} = 2L_{cb,j}\left[\cos(90° - \alpha_{b,j}) + \sqrt{\cos^2(90° - \alpha_{b,j}) + \frac{N_{cb,j}^{tar}}{E_{cb}A_{cb}}\left(\frac{N_{cb,j}^{tar}}{E_{cb}A_{cb}} + 2\right)}\right] \quad (11)$$

where $L_{cb,j}$ is the length of the bottom cables after deformation under the load $P_{LC,j}$ given by the formula

$$L_{cb,j} = \sqrt{\left(\sqrt{0{,}5L_s}\right)^2 + \left(d_b + w_j\right)^2} = \sqrt{0{,}5L_s^2 + \left(d_b + w_j\right)} = \sqrt{0{,}5L_s^2 + \left(0{,}5L_{AM,i} + w_j\right)^2} \quad (12)$$

where w_j is the vertical deflection at the midpoint of the tensegrity system under the load $P_{LC,j}$, $d_b = 0{,}5L_{AM,i}$ is the sag of the bottom cables and $L_{AM,i} = L_{AM0} + \Delta_{AM,i}$ is the length of the action member after the initial pre-stressing forces were introduced into the system (see Eq. (1)). The angle $\alpha_{b,j}$ is given by the formula

$$\alpha_{b,j} = \sin^{-1}\left(\frac{d_b + w_j}{L_{cb,j}}\right) = \sin^{-1}\left(\frac{0{,}5L_{AM,i} + w_j}{L_{cb,j}}\right) \quad (13)$$

Limits for vertical deflections can be specified for the tensegrity system. The approach also enables the setup of the system under the limit vertical deflection w_{lim} and to maintain this deflection under the specified limit value.

4 Experimental analysis of an adaptive tensegrity module

4.1 Characteristics of the test equipment

The special test equipment has been designed and manufactured to implement tests of a functionality and behaviour of the adaptive tensegrity system. The test equipment consists of a rigid self-supporting space frame structure into which the investigated tensegrity system and load cylinder are fitted, hydraulic power unit, control electronics, hardware and software.

The spatial self-supporting inverted steel frame has in plan a cross shape with outside dimensions of 3400×3400 *mm*, as is shown in Figure 8. The height of the structure is $1905\,mm$ and its weight is $520\,kg$. Horizontal members of the welded frame structure are made of rolled I sections 2 x IPN 200 (two I sections situated at each other) and vertical members (the four columns of the frame) are generated from a rolled section IPN 200. Between horizontal and vertical members are placed inclined braces of the frame corners. Short reinforced cantilevers on which is suspended the investigated tensegrity system are situated at the ends of the columns (Figure 8). A required stiffness of the frame has been verified by calculations. The frame is placed on the rubber pads.

The specially designed load cylinder, which can move simultaneously with the movement of the active member, is anchored in the middle of the bottom transversal beam of the frame as is shown in Figure 8. Thus, the load cylinder does not restrain in a movement of the actuator even if a loading force is applied.

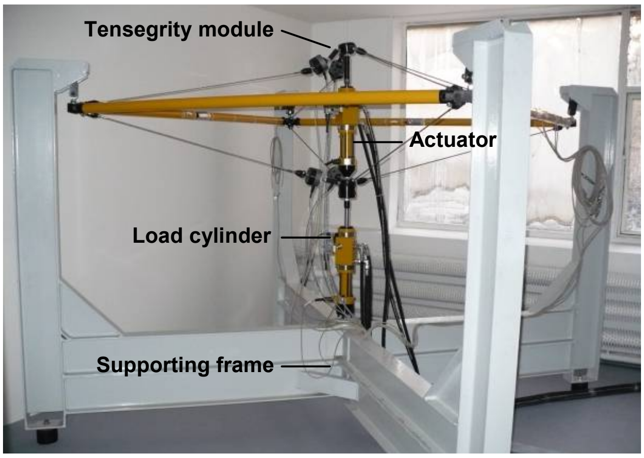

Figure 8: The tensegrity unit suspended on the self-supporting frame.

The load cylinder (LC) is a rectilinear hydraulic motor with inductive position sensor embedded in the piston rod. The maximum lift of the hydraulic motor is $100\ mm$ and the maximum nominal loading force, which can be generated, is $5\,kN$. Servo valves are used for a control of the load cylinder, which allow a generation of the required load P_{LC} through the movement Δ_{LC} of the piston. If the piston of the load cylinder retracts, a load of the tensegrity module increases and if the piston extends a load of the tensegrity module decreases.

4.2 Controlling unit, electronics and software

A management of tests on the electro-hydraulic equipment is carried out by the controlling unit CU 14 with the controlling electronics, which consists of a personal computer, the source block for the power of the regulators, a backup source, a specialized analogue-digital adapter ADAS 16 and a configuration of digital regulators RED 03.

Controlling software is a LabEXPERT program system, which creates the programming environment for an implementation of various types of quasi-static and dynamic tests. LabEXPERT contains several programs serving to operate the equipment by means of sensors that are assigned to the connected hardware and interactive graphical display of measured data. The LabEXPERT program allows an automated control of tests and an execution of control commands for an introduction of the initial pre-stressed state of the tensegrity system, for its loading and adaptation. The program provides an automatic communication with the attached facilities.

4.3 Characteristics and test results of the tensegrity system

Three types of the following tests were carried out: a pre-stressing test, a static loading test and an adaptation test.

The first test was aimed at the introduction and control of initial pre-stressing forces in tension cables of the tensegrity system through a movement of the action member under the zero loading. The pre-programmed fully automated block test with a duration of 140 seconds was carried out. By a progressive movement of the action member the corresponding levels of initial pre-stressing forces in the bottom and top cables of the tensegrity system were gradually generated. Course of the force F_{AM} in the action member at the time is shown in Figure 9a. Forces in the load cylinder during the test are equal to zero as can be seen from Figure 9b. Pre-stressing forces in the bottom cables (record from FT 1 and FT 2 transducers) and top cables (record from FT 3 and FT 4 transducers) of the tensegrity system increase by a gradual increase of forces in the action member under its elongation as is shown in Figure 10a and Figure 10b. Courses of the corresponding compression forces in the circumferential strut members at the time (record from SG 1, SG 5 and SG 6 strain gauges) are shown in Figure 11.

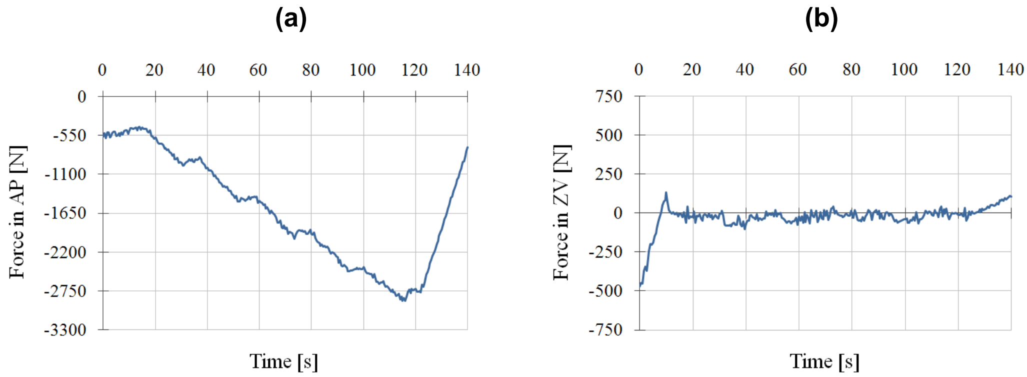

Figure 9: Change of the axial forces in the action member AM (a) and in the loading cylinder LC (b).

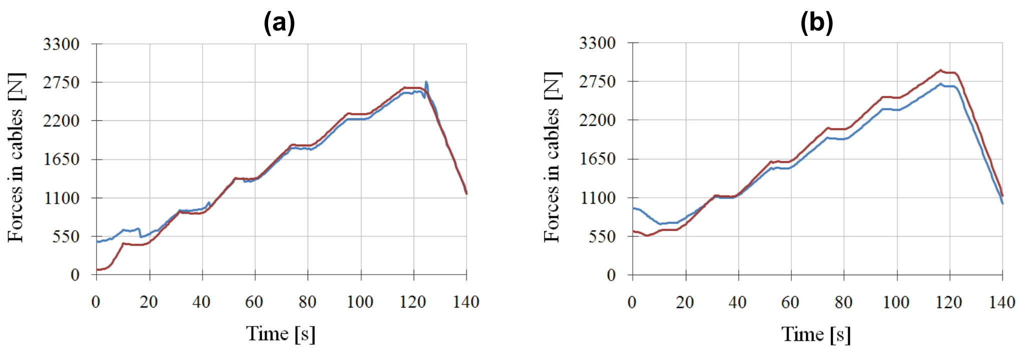

Figure 10: Forces in the bottom cables (a) and top cables (b).

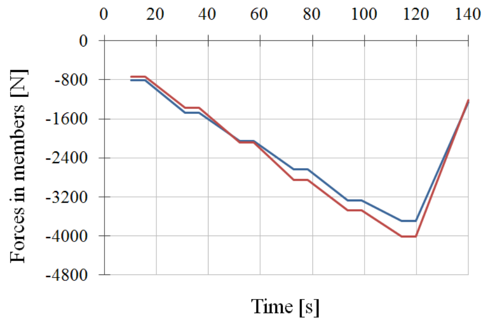

Figure 11: Forces in the compressed members.

The second test was aimed at the investigation of the behaviour of the initially pre-stressed tensegrity system under a gradual increase of the load. Duration of the pre-programmed fully automated block test was again 140 seconds.

The third test was aimed at a verification of the tensegrity system's ability to adapt its geometry and state of the stress to changing load cases in order to maintain reliability of the system. The aim was to prevent the slackening in the top cables of the tensegrity system. The fully automated block test with the duration of 140 seconds was pre-programmed as follows.

Tests confirmed the required functionality of the developed adaptive tensegrity system and the correctness of the proposed electronic equipment and software. An ability of the adaptability of the tensegrity system was demonstrated and proved. The required limit states criteria in the form of the limit tension forces in the bottom or top cables can be pre-programmed to the tensegrity system and the structure is able to automatically adjust its geometry and adapt its stress state to the current load conditions in order to satisfy the predefined reliability criteria.

5 Simplified closed-form solution of the tensegrity module

The diagonal geometrical and member symmetry of the 3D tensegrity module was used to develop the 2D closed-form static computational model for the equivalent system in the form of the hinge supported suspended biconvex triangular chord cable truss under a half point load, as is shown in Figure 12. A single cable truss is laterally stable under the influence of applied vertical loading because of the presence of the lateral bracing between adjacent trusses. This lateral bracing of the cable truss is modelled by hinge supports with a possible movement in the vertical direction located at places of the top and bottom node.

The profile geometry of the biconvex triangular chord cable truss is shown in Figure 12. Because of generality, consider the asymmetric cable truss about its longitudinal axis, i.e. trusses whose chord properties and profiles differ. The profiles of the bottom and top chords, respectively, are assumed to be linear and given by

$$z_{b1} = 2d_b \frac{x}{l} \text{ for } x \in \langle 0, l/2 \rangle, \; z_{b2} = 2d_b\left(1 - \frac{x}{l}\right) \text{ for } x \in \langle l/2, l \rangle$$

$$z_{t1} = 2d_t \frac{x}{l} \text{ for } x \in \langle 0, l/2 \rangle, \; z_{t2} = 2d_t\left(1 - \frac{x}{l}\right) \text{ for } x \in \langle l/2, l \rangle \qquad (14)$$

where l is the span of the triangular cable truss, d_b is the sag of the bottom carrying cable and d_t is the camber of the top stabilizing cable at the middle of the span.

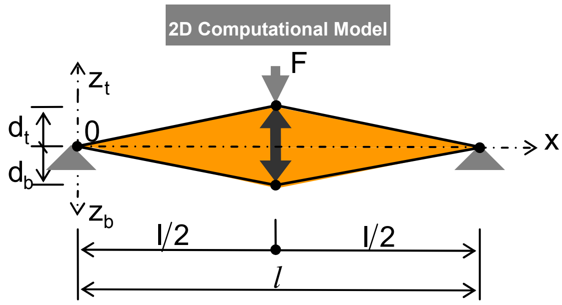

Figure 12: Definition diagram of a structure.

Differential equations of a vertical equilibrium at a cross section x of the biconvex cable truss obtain the form

$$(H_{0b}+H_{0t})\frac{dw_1}{dx}+\Delta H_b\frac{dz_{b1}}{dx}+\Delta H_t\frac{dz_{t1}}{dx}=\frac{P}{2} \quad \text{for } x\in\langle 0,l/2\rangle \text{, and}$$

$$(H_{0b}+H_{0t})\frac{dw_2}{dx}+\Delta H_b\frac{dz_{b2}}{dx}+\Delta H_t\frac{dz_{t2}}{dx}=-\frac{P}{2} \quad \text{for } x\in\langle l/2,l\rangle \tag{15}$$

where H_{0b} and H_{0t} are the horizontal components of the pretensions in the bottom and top chords, respectively, ΔH_b and ΔH_t are the additional horizontal components of cable tensions owing to the applied load, $z_{b1,2}$ and $z_{t1,2}$ are the initial profiles of the chords given by Equations (14), and $w_{1,2}$ is the additional vertical deflection in the corresponding part of the span.

The linear differential equations (15) may be integrated directly, and after the boundary conditions have been applied, the equations for the vertical deflection of a biconvex cable system are obtained in the forms

$$w_1=\frac{1}{(H_{0b}+H_{0t})}\left(\frac{P}{2}x-\Delta H_b\frac{2d_b}{l}x-\Delta H_t\frac{2d_t}{l}x\right) \quad \text{for } w_1\in\langle 0,l/2\rangle \text{, and}$$

$$w_2=\frac{1}{(H_{0b}+H_{0t})}\left(\frac{Pl}{2}-\frac{P}{2}x-\Delta H_b 2d_b\left(1-\frac{x}{l}\right)-\Delta H_t 2d_t\left(1-\frac{x}{l}\right)\right) \text{for } w_2\in\langle l/2,l\rangle \tag{16}$$

The linear cable equations are

$$\frac{\Delta H_b L_{eb}}{E_b A_b}=\int_0^{l/2}\left(\frac{dz_{b1}}{dx}\right)\left(\frac{dw_1}{dx}\right)dx+\int_{l/2}^{l}\left(\frac{dz_{b2}}{dx}\right)\left(\frac{dw_2}{dx}\right)dx$$

$$\frac{\Delta H_t L_{et}}{E_t A_t}=\int_0^{l/2}\left(\frac{dz_{t1}}{dx}\right)\left(\frac{dw_1}{dx}\right)dx+\int_{l/2}^{l}\left(\frac{dz_{t2}}{dx}\right)\left(\frac{dw_2}{dx}\right)dx \tag{17}$$

where E_b and E_t are the modules of elasticity of the bottom and top chords, respectively, and A_b and A_t are the cross-sectional areas of the cable chords. Substituting the deflection equations (16) into Equations (17) and performing the necessary integration, the following coupled system of two linear cable equations for unknown ΔH_b and ΔH_t is found as

$$\left(\frac{L_{eb}}{E_b A_b}(H_{0b}+H_{0t})l+4d_b^2\right)\Delta H_b+4d_b d_t \Delta H_t=Pd_b l$$

$$4d_b d_t \Delta H_b+\left(\frac{L_{et}}{E_t A_t}(H_{0b}+H_{0t})l+4d_t^2\right)\Delta H_t=Pd_t l \tag{18}$$

The simultaneous solution of Equations (18) produces the results in the explicit form

$$\Delta H_b=\frac{Pd_b l}{\frac{L_{eb}}{E_b A_b}\left((H_{0b}+H_{0t})l+4d_b^2\frac{E_b A_b}{L_{eb}}+4d_t^2\frac{E_t A_t}{L_{et}}\right)}$$

$$\Delta H_t=\frac{Pd_t l}{\frac{L_{et}}{E_t A_t}\left((H_{0b}+H_{0t})l+4d_b^2\frac{E_b A_b}{L_{eb}}+4d_t^2\frac{E_t A_t}{L_{et}}\right)} \tag{19}$$

The deflection equations (16) and the expressions (19) are sufficient to obtain linear closed-from solutions for the dependent variables $w_{1,2}$, ΔH_b and ΔH_t. In general, a deflection response will be slightly overestimated, which is conservative, while an additional tension in the bottom bearing cable will be underestimated in these linear solutions.

6 Finite-element analysis of an adaptive tensegrity module

A finite element method was used to study the behaviour of the adaptive tensegrity system and to compare the calculated simulated response with experimental values obtained from the individual tests. The method is also employed to assess the results obtained through the developed closed-form solution. The nonlinear analyses were conducted by using the ANSYS 12 Classic finite-element software package [17].

6.1 Finite-element modelling

Two-node rectilinear spatial elements with three degrees of freedom at each node (displacements in the nodal x, y and z directions) marked as LINK 10 and LINK 11 in the ANSYS 12 Classic library were used for the analyses of the adaptive tensegrity module.

The LINK 10 element was used to model the tension cables and compressed rods. LINK 10 is a three-dimensional spar element having the unique feature of a bilinear stiffness matrix resulting in a uniaxial tension-only or compression-only element. With the tension-only option, the stiffness is removed if the element goes into compression (simulating a slack cable). This feature is useful for cable applications where the entire cable is modelled with one element. The material model for the cables and struts is characterized by a linear relationship between stresses and strains (physical linearity), hence Hooke's law is valid for their behaviours in the elastic range.

The LINK 11 linear actuator was used to model the action member. LINK 11 is a uniaxial tension-compression element with three degrees of freedom at each node: translations in the nodal x, y, and z, directions. No bending or twist loads are considered. The geometry and node locations for the element are shown in Figure 13. The element is defined by two nodes, a stiffness K, viscous damping C, and mass m. The element initial length L_0 and orientation are determined from the node locations.

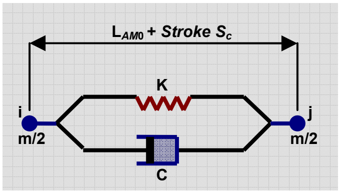

Figure 13: LINK 11 element.

6.2 Nonlinear FEM analysis

The updated Lagrangian formulation is applied to solve geometric nonlinear tasks. For the updated Lagrangian approach, the discrete equations are formulated for the current configuration, which is assumed to be the new reference configuration.

The solution of this system of nonlinear equations is typically accomplished with an iterative method. The load vector is subdivided into a number of sufficiently small load increments. At the finishing point of each incremental solution, the stiffness matrix of the model is adjusted to reflect nonlinear changes in structural stiffness before proceeding to the next load increment. The ANSYS program uses Newton-Raphson equilibrium iterations for updating the model stiffness. Newton-Raphson equilibrium iterations provide convergence at the end of each load increment within tolerance limits. The finite element discretization process yields a fundamental system of non-linear equilibrium equations

$$[K_T]\{w\} = \{P\} \tag{20}$$

where $[K_T]$ is the tangent stiffness matrix, $\{w\}$ is the vector of unknown nodal displacements and $\{P\}$ is the vector of applied loads. A conservative load is considered in the solution, thus a load vector $\{P\}$ is configured for the initial state of the structure and its direction is not changed during the calculation.

Tangential stiffness matrix $[K_T] = [K_E] + [K_G]$ of the LINK 10 element consists of an elastic stiffness matrix and geometric stiffness matrix. The elastic and geometric stiffness matrix of the LINK 11 active element has the form

$$[K_{E,AM}] = K_{AM}\begin{bmatrix} M_E & -M_E \\ -M_E & M_E \end{bmatrix} \tag{21}$$

$$[K_{G,AM}] = \frac{K_{AM}(S_C - S_{AM})}{L}\begin{bmatrix} M_G & -M_G \\ -M_G & M_G \end{bmatrix} \tag{22}$$

where K_{AM} is the stiffness of the active element, S_{AM} is the applied stroke of the active element through the internal force introduction into the active member and S_C is the calculated or measured elongation (stroke) of the element.

The mass matrix $[M_{AM}]$ and the damping matrix $[C_{AM}]$ of an active element have the forms

$$[M_{AM}] = \frac{m}{2}\begin{bmatrix} M_m & M_0 \\ M_0 & M_m \end{bmatrix} \tag{23}$$

$$[C_{AM}] = C\begin{bmatrix} M_c & -M_c \\ -M_c & M_c \end{bmatrix} \tag{44}$$

where m is the mass of the active member and C is the viscous damping coefficient. Auxiliary matrices used in the previous expressions have the forms

$$M_E = M_C = \begin{bmatrix} 1 & 0 & 0 \\ 0 & 0 & 0 \\ 0 & 0 & 0 \end{bmatrix} \quad M_G = \begin{bmatrix} 0 & 0 & 0 \\ 0 & 1 & 0 \\ 0 & 0 & 1 \end{bmatrix} \quad M_m = \begin{bmatrix} 1 & 0 & 0 \\ 0 & 1 & 0 \\ 0 & 0 & 1 \end{bmatrix} \quad M_0 = \begin{bmatrix} 0 & 0 & 0 \\ 0 & 0 & 0 \\ 0 & 0 & 0 \end{bmatrix} \tag{25}$$

The incremental Newton-Raphson procedure is applied to solve Equations (20). This procedure is ideally suited for the solution of geometric nonlinear tasks and its effectiveness has been demonstrated by a number of numerical examples.

Boundary conditions were set for all supporting points of the tensegrity system. The supporting nodes (at the corner nodes of the square base) can move (displace) in horizontal directions (displacements in the direction of x-axis and z-axis) but their vertical displacement is restrained (displacement in the direction of y-axis). The top and bottom node of the system can move in all directions.

Time dependent tasks connected with the control and adaptation of the tensegrity module were simulated through the non-linear transient dynamic analysis (sometimes called time-history analysis) in the time domain [17].

The basic equation of motion solved by a transient dynamic analysis is

$$[M]\{\ddot{w}\} + [C]\{\dot{w}\} + [K_T]\{w\} = \{F^{appl}(t)\} \tag{37}$$

where $[K_T] = [K_E] + [K_G]$ is the tangential stiffness matrix, $[C]$ is the damping matrix, $[M]$ is the mass matrix, $\{w\}$ is the nodal displacement vector, $\{\dot{w}\}$ is the nodal velocity vector, $\{\ddot{w}\}$ is the nodal acceleration vector and $\{F^{appl}(t)\}$ is the applied load vector. To solve these equations at discrete time points the Newmark time integration method was applied.

7 Comparison of experimental and theoretical results

In this section, the experimental results described in the paper are used to validate the proposed computational models.

In order to compare the results, the equivalent conditions for the adaptive tensegrity system with the corresponding geometric and material properties have been generated in the analytical and numerical models for the individual types of the tests. The initial pre-stresses of the system with the adequate loading programs, and their changes corresponding to the conditions during the individual tests were considered. A finite-element model of the active tensegrity module with the characteristic element is shown in Figure 14. For the form-finding of the initial shape and pre-stress of the tensegrity module the dynamic relaxation method was used [18].

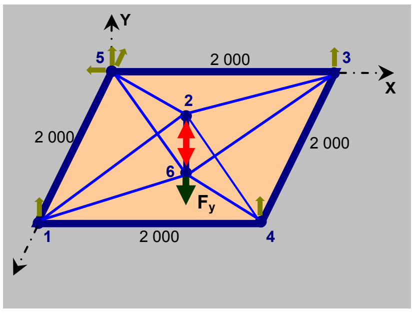

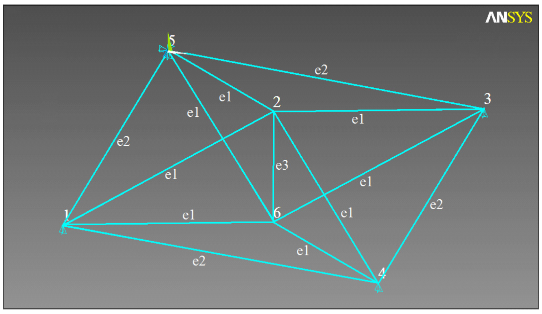

Figure 14: A finite-element model of the active tensegrity module. LINK10: tension-only spar element (**e1**) for the cables, LINK10: compression-only spar element (**e2**) for the compressed members and LINK11: linear actuator (**e3**) for the active member (AM).

Following figures give a full comparison of experimental, analytical, and numerical results covering the key response parameters as were obtained from the three mutually independent tests of the tensegrity module: a pre-stressing test, a static loading test and an adaptation test.

Comparison of the experimentally and theoretically obtained values of the change of the force in the action member, in the load member, in the bottom cable members, in the top cable members and in the circumferential compressed rods at the time, are shown in the case of the 1st test (a pre-stressing test) in Figure 15, Figure 16 and Figure 17.

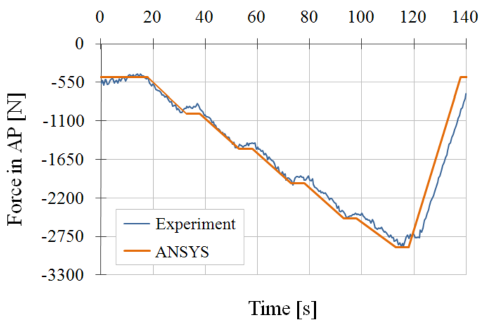

Figure 15: Course of changes of the axial forces in the action member.

Results confirmed a physical relevance and logical correctness of the applied theoretical approaches.

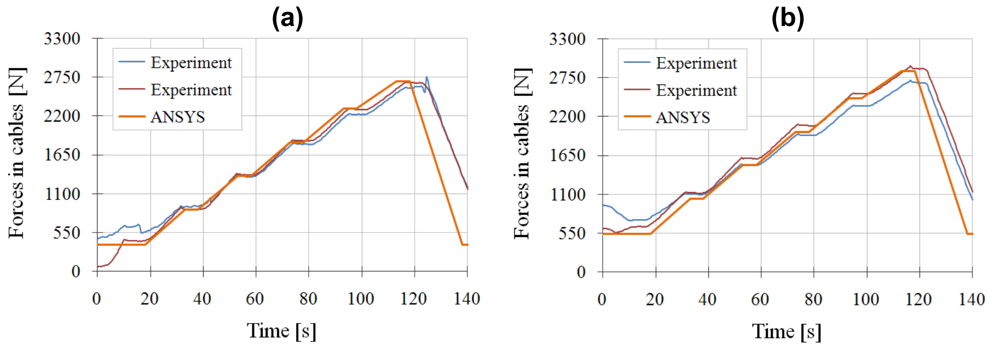

Figure 16: Forces in the bottom cables (a) and in the top cables (b).

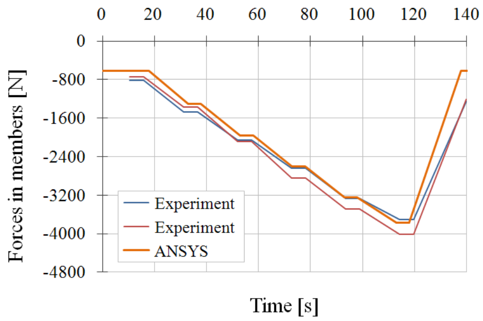

Figure 17: Forces in the compressed members.

8 Conclusion

A developed newly adaptive tensegrity system which has the ability to alter its geometrical form and stress properties in order to adapt its behaviour in response to the current loading conditions was presented in this paper. Results of the experimental and theoretical analyses of the developed adaptive tensegrity system were presented. Tests confirmed the required functionality of the developed adaptive tensegrity system and the correctness of the proposed electronic equipment and software. An ability of the adaptability of the tensegrity system was demonstrated and proved. The required limit states criteria in the form of the limit tension forces in the bottom or top cables can be pre-programmed to the tensegrity system and the structure is able to automatically adjust its geometry and adapt its stress state to the current load conditions in order to satisfy the predefined reliability criteria.

To increase the reliability and enhance the performance of tensegrity structures: that is why this new approach is useful. It is believed that the adaptive tensegrity system presented will create a basis for new technology for a variety of civil engineering applications.

Acknowledgements

This work is a part of Research Project No. 1/12, partially founded by the Scientific Grant Agency of the Ministry of Education of Slovak Republic and the Slovak

Academy of Sciences. The present research has been carried out within the project Centre of excellent integrated research of the progressive building structures, materials and technologies, supported from the Structural funds of the European Union.

References

[1] R.B. Fuller, "*Synergetics explorations in the geometry of thinking",* Collier Macmillan Publishers, London, 1975.

[2] A. Pugh, "*An introduction to tensegrity",* Berkley, CA: University of California Press, Berkley, USA, 1976.

[3] R.Motro, "*Tensegrity: Structural systems for the future",* Hermes, ed., Penton Science, U.K., 2003.

[4] R.E. Skelton, M.C. de Oliveira, "*Tensegrity systems",* Springer Science and Business Media, New York, 2009.

[5] H. Murakami, Y. Nishimura, "Initial shape finding and modal analyses of cyclic right-cylindrical tensegrity modules", *Computers and Structures*, 79(9), 891-917, 2001.

[6] L. Zhang, B. Maurin, R. Motro, "Form-finding of nonregular tensegrity systems", *Journal of Structural Engineering*, ASCE, 132(9), 1435-1440, 2006.

[7] J. Rieffel, F. Valero-Cuevas, H. Lipson, "Automated discovery and optimization of large irregular tensegrity structures", *Computers and Structures*, 87(5-6), 368-379, 2009.

[8] H.C. Tran, J. Lee, "Advanced form-finding of tensegrity structures", *Computers and Structures*, 88(3-4), 237-246, 2010.

[9] X. Xu, Y. Luo, "Multistable tensegrity structures", *Journal of Structural Engineering*, 137(1), 117-123, 2011.

[10] G. Tibert, "Deployable tensegrity structures for space applications", PhD thesis, Dept. of Mechanics, Royal Inst. of Technology, Stockholm, Sweden, 2002.

[11] M. Saitoh, A. Okada, H. Tabata, "Study on the structural characteristics of tensegric truss arch. On structural characteristics of tensegric truss structure (Type I) in consideration of slack of strings", *Proc., Int. Symp. on Theory, Design and Realization of Shell and Spatial Structures*, H. Kunieda, ed., Nagoya, Japan, 326–327, 2001.

[12] M. Wu, M. Sasaki, "Structural behaviors of an arch stiffened by cables", *Engineering Structures*, 29(4), 529-541, 2007.

[13] K. Shea, E. Fest, I.F.C. Smith, "Developing intelligent tensegrity structures with stochastic search", *Advanced Engineering Informatics*, 16(1), 21-40, 2002.

[14] E. Fest, K. Shea, B. Domer, I.F.C. Smith, "Adjustable tensegrity structures", tensegrity structures", *Journal of Structural Engineering*, 129(4), 515-526, 2003.

[15] E. Fest, K. Shea, I.F.C. Smith, "Active tensegrity structure", *Journal of Structural Engineering*, 130(10), 1454-1465, 2004.
[16] Eurocode 3, "*Design of steel structures. Part 1.11 Design of structures with tension components*", CEN, Brussels, 2006.
[17] ANSYS, Inc., "*Release documentation of Ansys 11.0*", Southpointe, 275 Technology Drive, Canonsburg, 2005.
[18] B.H.V. Topping, P. Ivanyi, "*Computer aided design of cable membrane Structures"*, Saxe-Coburg Publications, Stirlingshire, Scotland 2007.